Ground-state geometries and stability of impurity doped clusters: Li_nBe and Li_nMg ($n=1-12$)

M. Deshpande,* A. Dhavale,† R. R. Zope,‡ S. Chacko,§ and D. G. Kanhere‖
Department of Physics, University of Pune, Pune 411 007, India
(Received 9 June 2000; published 8 November 2000)

We have investigated the ground-state geometries of Li_nBe and Li_nMg ($n=1-12$) clusters using *ab initio* molecular dynamics. These divalent impurities Be and Mg induce different geometries and follow a different growth path for $n>5$. Li_nMg clusters are significantly different from the host geometries while Li_nBe clusters can be approximately viewed as Be occupying an interstitial site in the host. Our results indicate that Be gets trapped inside the Li cage, while Mg remains on the surface of the cluster. Mg-induced geometries become three-dimensional earlier at $n=4$ as compared to the Be system. In spite of a distinct arrangement of atoms in both cases the character of the wave functions in the *d* manifold is remarkably similar. In both cases an eight valence electron system has been found to be the most stable, in conformity with the spherical jellium model.

PACS number(s): 36.40.Qv, 36.40.Mr, 61.46.+w, 31.15.Ar

I. INTRODUCTION

The ground-state geometries, energetics, stability, and other such properties of clusters are the subject of intensive investigation [1]. Apart from serving as a prototype for understanding the nanosized and cluster-assembled materials, clusters exhibit many interesting properties that are neither atomiclike nor extended solidlike. One of the interesting aspects of the study is the size dependence of geometries, energetics, and stability. Such studies have already revealed novel properties like magic clusters. Although the gross features related to their stability can be understood from the spherical jellium model (SJM) [2,3], more sophisticated theoretical methods are required to understand the details of the geometry which are essential to understanding properties like polarizability, photoelectron spectra, vibrational frequency, and melting phenomenon, etc. After the advent of the Car-Parrinello (CP) and related methods, *ab initio* density-functional molecular dynamics (DFMD) [4] is used as a standard tool for such investigations.

Although a number of investigations have been carried out on small homogeneous clusters, relatively few reports are available on heterogeneous systems. Much insight can be gained by examining the effect of a single impurity on the geometries of pure clusters. Here, we are reporting on the ground state and some low-lying geometries, energetics, and stability of Li_nBe and Li_nMg ($n=1-12$) clusters where a divalent impurity is doped in a monovalent host. There have been a few reports on such impurity induced clusters. Hai-Ping *et al.* [5] investigated the electronic structure of a trivalent impurity Al in Li_n clusters. They have found that smaller clusters show covalent bonding and charge density becomes delocalized with the size of the system. Dhavale *et al.* [6,7] investigated the electronic structure and stability of Na_n clusters with Al and Mg as impurities. They showed that Al gets trapped at $n=6$ while Mg gets trapped at $n=11$. There is an early appearance of a three-dimensional structure as compared to the host system. In all the above cases there is a reversal of the level order as compared to SJM, viz., the pattern evolves as $1s,1p,2s,1d$. Some electronic structure calculations have also been reported on Li_nMg [8], and Na_nMg [9,10] clusters. These few reports already indicate that impurity-induced geometries are dependent on ionic radii, valency of the impurity, and the nature of the impurity-host bonding. Therefore, we have carried out a systematic investigation of the ground-state geometries and energetics of divalent impurities Be and Mg in the monovalent host Li_n ($n=1-12$). Calculations have been carried out by using standard *ab initio* molecular dynamics with simulated annealing strategy. It may be noted that there have been earlier reports on these clusters by Fantucci *et al.* [11,12] and Pewestorf *et al.* [13] using the self-consistent-field–configuration-interaction method (SCF-C) but without the simulated annealing method. Our ground-state geometries, especially for the Mg systems, are found to be very different than reported in their work.

In Sec. II, we describe in brief the computational method and some numerical details. In Sec. III we present and discuss our results.

II. COMPUTATIONAL DETAILS

Most of the simulations have been carried out using the Car-Parrinello molecular-dynamics (CPMD) method. In a few cases, especially for larger systems showing metallic behavior, i.e., having a number of near-degenerate states, it was found convenient to use Born-Oppenheimer molecular dynamics. We have used the damped Joannopoulos method [14] for this purpose. This has permitted us to use a fairly moderate time step ≈ 100 a.u.

The geometries of a given cluster have been obtained by starting with unbiased configuration and then heating it to 600–800 K which is then followed by slow cooling. For those systems where the impurity atom was trapped in a Li

*Email address: mdd@physics.unipune.ernet.in
†Email address: ajd@physics.unipune.ernet.in
‡Present address: CEA, Grenoble, 17 rue des Martyrs, F-38054 Grenoble Cedex, France. Email address: rzope@cea.fr
§Email address: chacko@physics.unipune.ernet.in
‖Email address: kanhere@physics.unipune.ernet.in

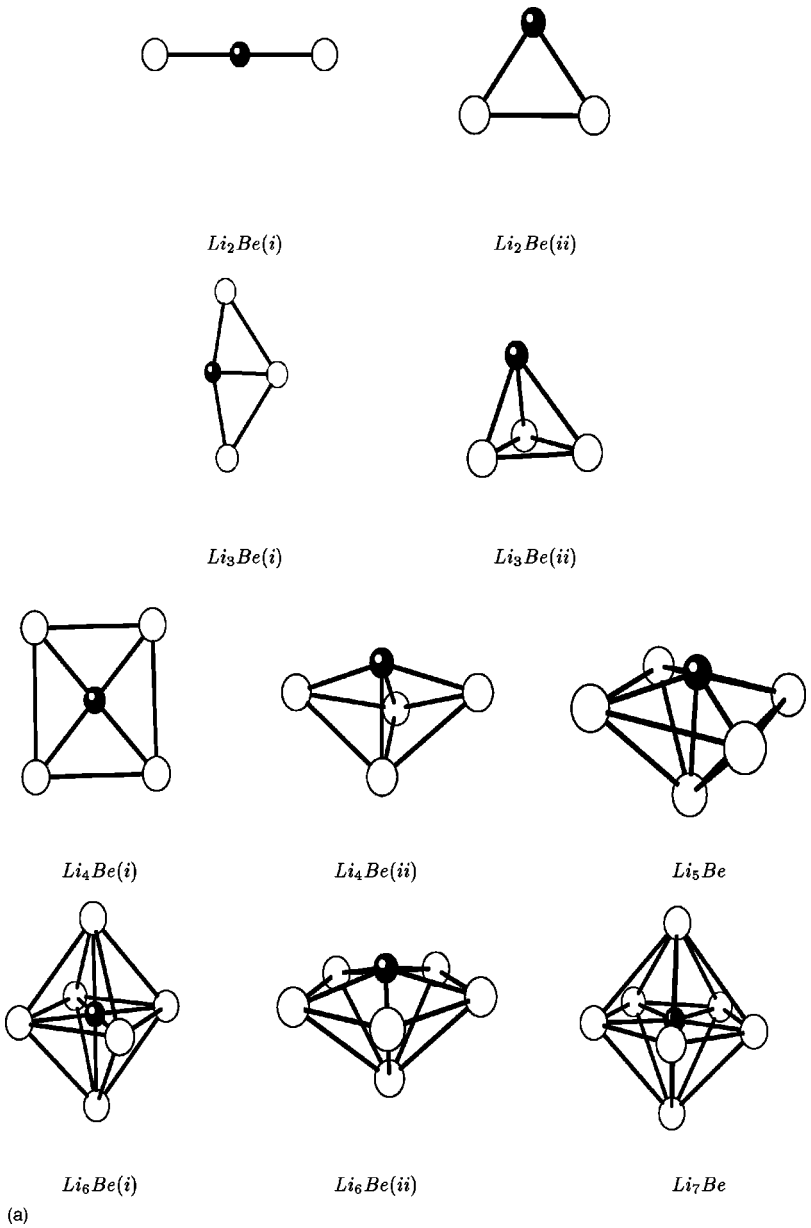

FIG. 1. The ground state and some low-lying geometries of Li_nBe clusters (a) $n=1$–6, (b) $n=7$–12. The dark circle represents the Be atom and the white circle the Li atom. (i) and (ii) indicate ground-state and low-lying structures of the cluster.

cage, the procedure was repeated with a different geometry having an impurity atom on the surface of the cluster. In all cases, the stability of the ground state and excited-state configurations has been tested by reheating the cluster and allowing it to span the configuration space, and then cooling it to get the lowest-energy configuration. We have used a norm-conserving nonlocal pseudopotential of Bachelet, Hamann, and Schluter with a p component taken as local and the Barth-Hedin exchange-correlation potential. All the calculations are carried out on a periodic cell of length 40 a.u. with the energy cutoff at approximately 11 Ry.

During the Born-Oppenheimer dynamics, the norm of each of the states defined as $|h\psi_i-\epsilon_i\psi_i|^2$ is maintained at 10^{-7} (where ϵ_i is an eigenvalue corresponding to state ψ_i of Hamiltonian h). The ground-state geometries were considered to be converged when the forces on all atoms were less than 10^{-4} a.u. The convergence of total energies and bond lengths was checked by varying the energy cutoff and the cell volume. The above parameters were found suitable.

III. RESULTS

In this section we present the results for the ground-state and some low-lying geometries, energetics, and stability for the series Li_nBe and Li_nMg clusters ($n=1$–12) The ground-state and some of the low-lying geometries for both the series are shown in Figs. 1(a) and 1(b) and 2(a), and 2(b), respectively, where the impurity atom Be/Mg is represented by a black sphere. While discussing the cluster geometries in the text, the symmetry of the geometry is mentioned in the

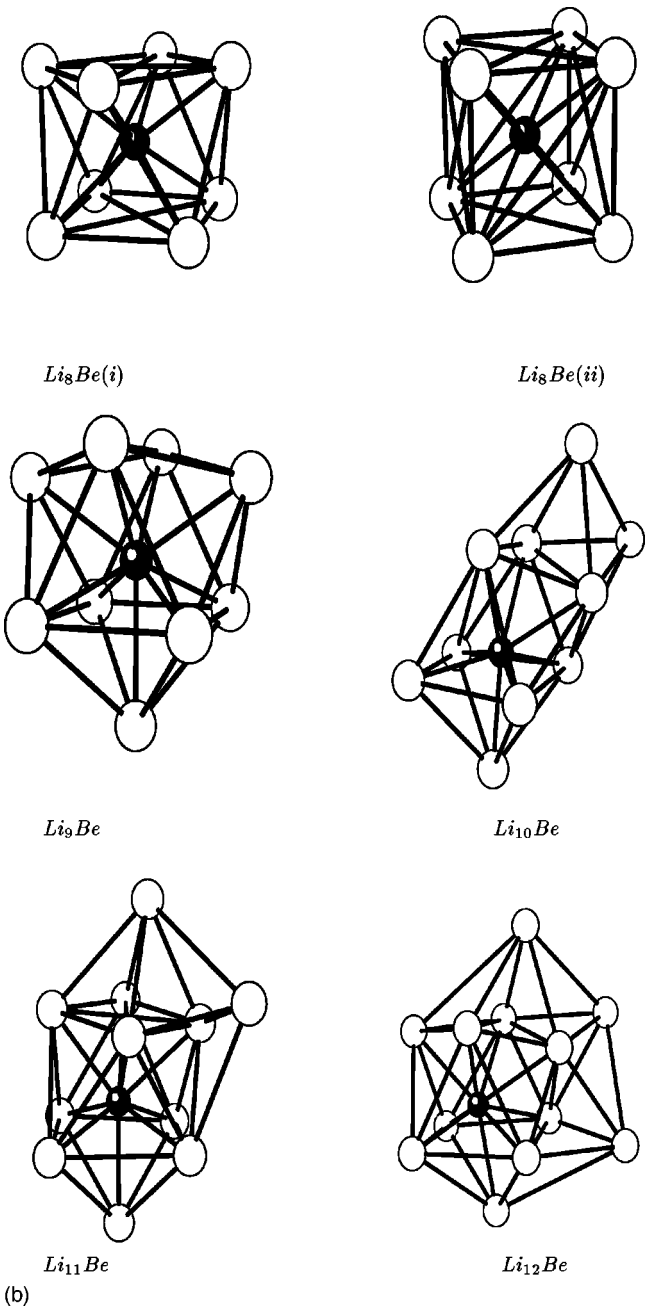

FIG. 1. (*Continued*).

parentheses. First, we will discuss the general features observed for Li_nBe and compare them with host systems Li_n [15,16].

The ground state of the three-atoms system (Li_2Be) turns out to be linear even though Li_3 is a triangle. The isosceles triangle (C_{2V}) is one of the low-lying structures at slightly higher energy. The ground state of Li_3Be is a planar kite like (C_{2V}) geometry and can be viewed as a distorted Li_4 structure where Be impurity substitutes one Li atom. One of the low-lying structures is a three-dimensional tetrahedron (C_{3V}). The lowest-energy state of Li_4Be is a planar square (D_{4h}), with a Be atom at the center of the square. The low-lying structure is a three-dimensional tetrahedron with a Be atom at the corner of the base and not at the most symmetric apex position. The addition of one more Li atom generates a regular square pyramid (C_{4V}) with a Be atom at its vertex. This is the first three-dimensional ground state in this series. It may be noted that in the case of Li_n, a three-dimensional structure occurs at $n=7$. This is expected from SJM where the appearance of a three-dimensional structure is related to the occupancy of the p_z orbital. Li_6Be (number of electrons $N_e=8$) is found to be the most stable system with the ground-state geometry as a regular octahedron (O_h). A pentagonal bipyramid (C_{5V}) with an impurity atom at one of the apex is one of the low-lying structures. From this cluster onwards the impurity is seen to be trapped in a Li cage. Li_7Be is a pentagonal bipyramid (D_{5h}), derived from the low-lying structure of Li_6Be. The addition of one Li atom does not retain the pentagonal ring. We obtain two structures for Li_8Be. The first one is an archimedian antiprism (D_{4d}), which is the lowest-energy structure where the impurity atom is slightly shifted from the center of mass, and the second one is the centered cubic (D_h). Li_9Be can be viewed as a capped archimedian antiprism (D_{3h}) accompanied by distortion. This trend of capping and distortion continues up to $n=12$. In addition, the tendency for the formation of a pentagonal ring is also evident. The structure of $Li_{12}Be$ reorganizes to regain partial spherical symmetry over $Li_{10}Be$ and $Li_{11}Be$ and can be viewed as a distorted icosahedron.

Now we present the geometries of Li_nMg and contrast their growth patterns with that of Li_nBe clusters. The ground-state geometries of both the impurity systems are similar for $n \leqslant 5$ except for $n=4$ where Mg-induced structures are reversed as compared to Li_4Be. In this case the ground state is tetrahedron (C_{3V}). Interestingly the first three-dimensional structure appears for a six-electron system instead of a seven-electron system. This indicates that the highest occupied molecular orbit (HOMO) state, i.e., the third state, has significant p_z character (see the discussion at the end of this section). The growth patterns of Li_nMg structures from $n \geqslant 6$ is significantly different than Li_nBe. These structures evolve by successive capping of Li on one of the faces of the octahadra of Li_5Mg. It is also observed that from $n=8$ to $n=10$ fourfold-coordinated ring distorts towards a pentagonal ring. Further, even at $n=12$, Mg is not trapped inside the cage but is a part of a pentagonal ring. In each case the geometry with trapped impurity is at a higher energy.

Thus, it can be seen that the Be atom gets trapped in the Li cage for $n>5$ while the Mg atom remains on the surface of the cluster. The trapping of an impurity atom can be understood on the basis of atomic radius of constituent atoms and the relative strength of the bond between them. The ionic radius of Mg (1.36 Å) is larger than Li (1.25 Å) while Be (0.89 Å) is substantially smaller than Li. Further, the Li—Be bond (0.391 eV) is stronger than the Li—Mg bond (0.263 eV). This makes it harder for Mg to go inside. In other words, the cluster minimizes energy by maximizing Li—Li bonds (0.807 eV).

A comparison of ground-state geometries with the re-

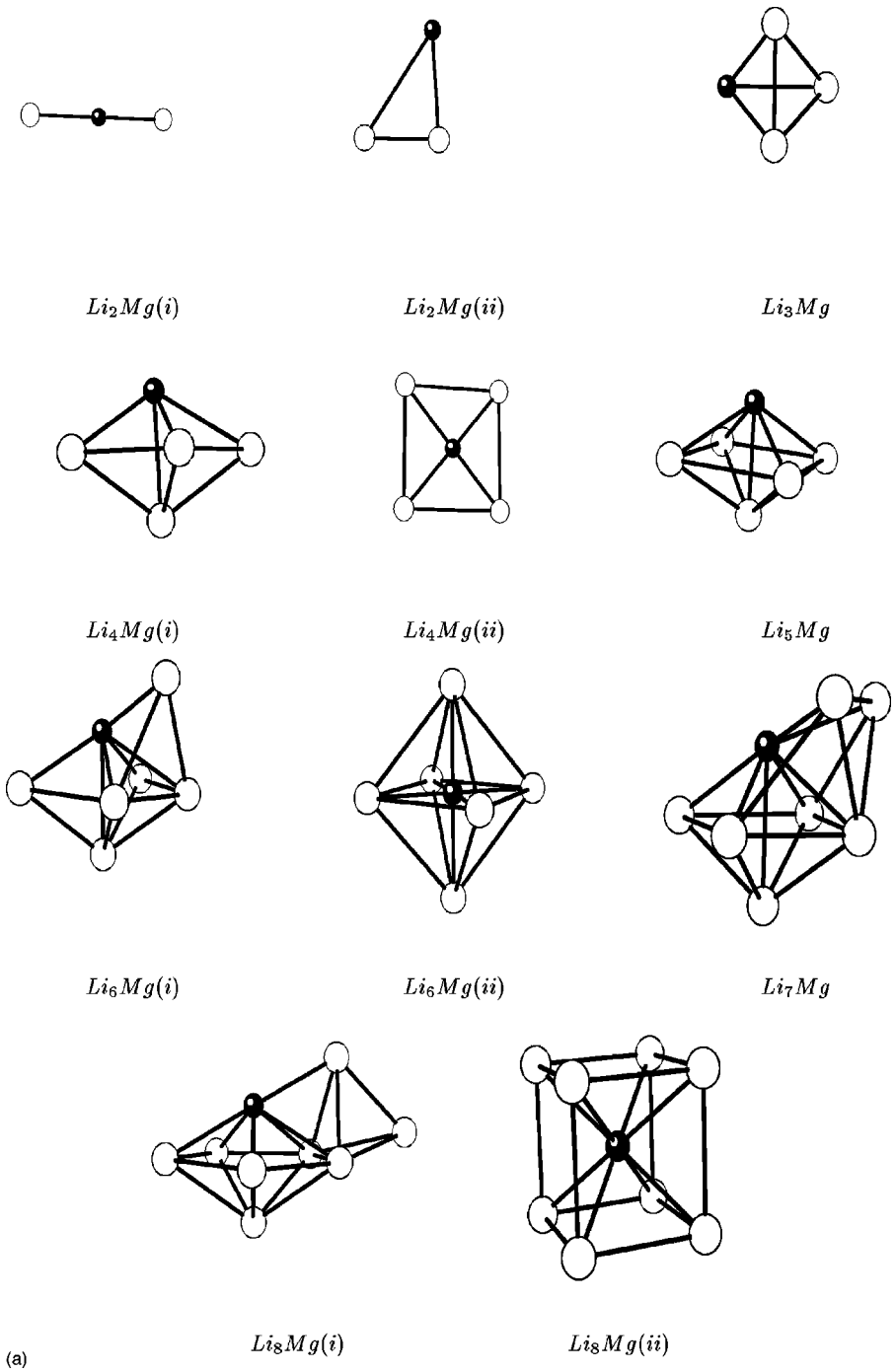

FIG. 2. The ground state and some low-lying geometries of Li_nMg clusters (a) $n=1-8$, (b) $n=9-12$. The dark circle represents the Mg atom and the white circle the Li atom. (i) and (ii) indicate ground-state and low-lying structures of the cluster.

ported results of Fantucci *et al.* [11,12] and Pewestorf *et al.* [13] brings out some noteworthy differences. We first note that they have used the SCF-CI technique but without the simulated annealing method which amounts to obtaining a local minimum only. Our results for Li_nBe geometries are similar to their geometries except for $n=5$ and 8. For $n=5$ we get a three-dimensional structure while their [11–13] geometry is planar. In our case for an $n=8$ centered cube is at higher energy by (0.01 eV) while it is their lowest-energy state. In the case of Li_nMg our ground-state geometries are totally different than reported by them [11–13] for $n>3$. In their case Mg is seen to be trapped in a Li_n cluster which is contradictory to our results. In their case both the impurity-induced structures are very similar. These differences are clearly due to simulated annealing strategy used in the present work.

The stability of these clusters can be discussed on the basis of binding energies per atom (E_b), dissociation

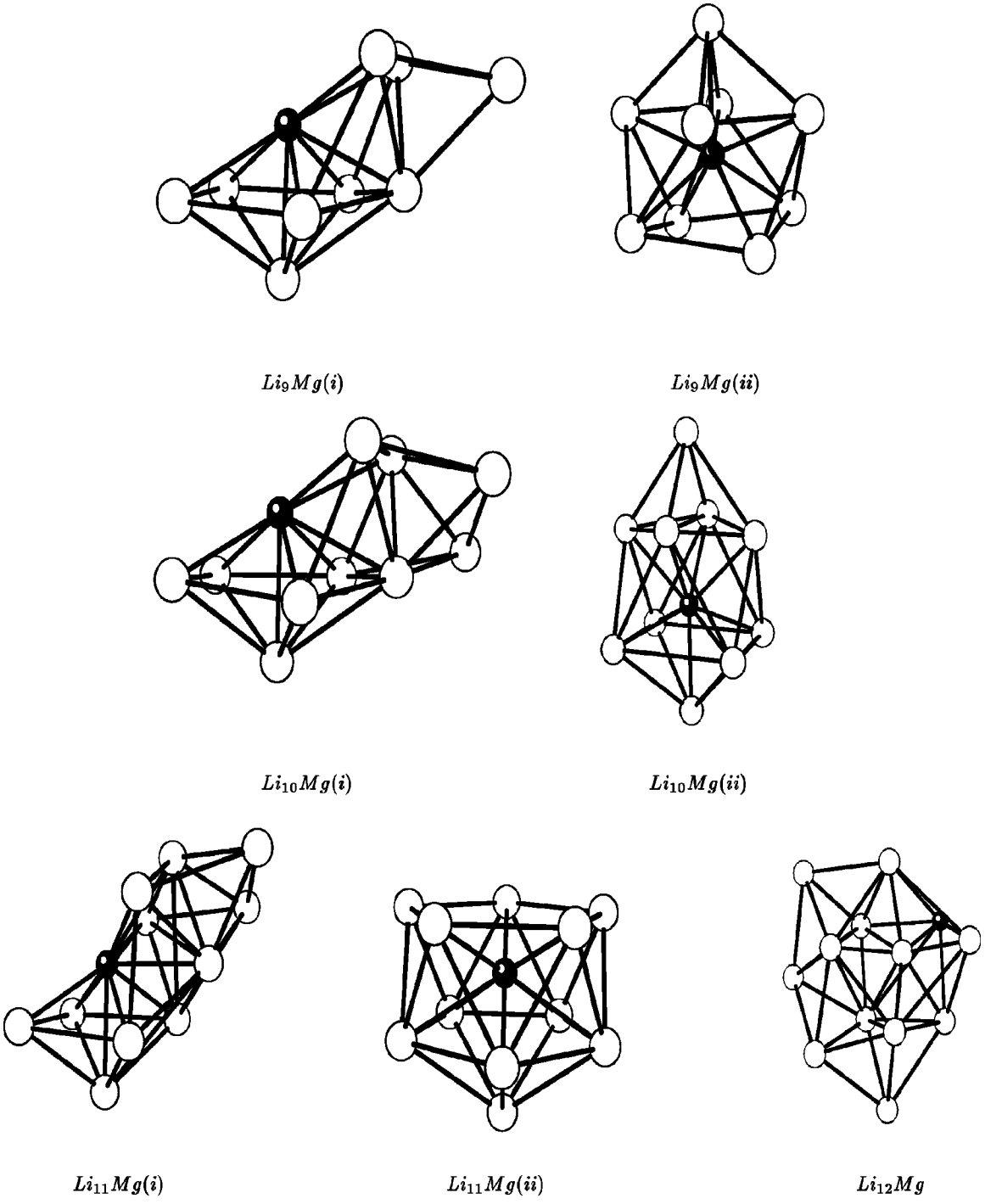

FIG. 2. (*Continued*).

energies (ΔE), and second differences in energies ($\Delta^2 E$), where

$$E_b[\mathrm{Li}_n\mathrm{Be}] = (-E[\mathrm{Li}_n\mathrm{Be}] + nE[\mathrm{Li}] + E[\mathrm{Be}])/(n+1),$$

$$\Delta^2 E[\mathrm{Li}_n\mathrm{Be}] = -2E[\mathrm{Li}_n\mathrm{Be}] + E[\mathrm{Li}_{n+1}\mathrm{Be}] + \mathrm{E}[\mathrm{Li}_{n-1}\mathrm{Be}],$$

$$\Delta E[\mathrm{Li}_n\mathrm{Be}] = E[\mathrm{Li}_n\mathrm{Be}] - (E[\mathrm{Li}_{n-1}\mathrm{Be}] + E[\mathrm{Li}]),$$

where E is the total energy of the system.

The binding energies per atom (in eV) for $\mathrm{Li}_n\mathrm{Be}$ and $\mathrm{Li}_n\mathrm{Mg}$ clusters are plotted against the total number of atoms in Fig. 3(a). The plot indicates that $\mathrm{Li}_n\mathrm{Mg}$ is comparatively a weakly bound system. The highest binding is observed at $N_e = 8$. This stability is brought out by the behavior of second differences and dissociation curves. We show the second difference in energy and the dissociation energy for $\mathrm{Li}_n\mathrm{Be}$ in Fig. 3(b) and for $\mathrm{Li}_n\mathrm{Mg}$ in Fig. 3(c). Both the curves show the even-odd pattern. This also indicates that apart from

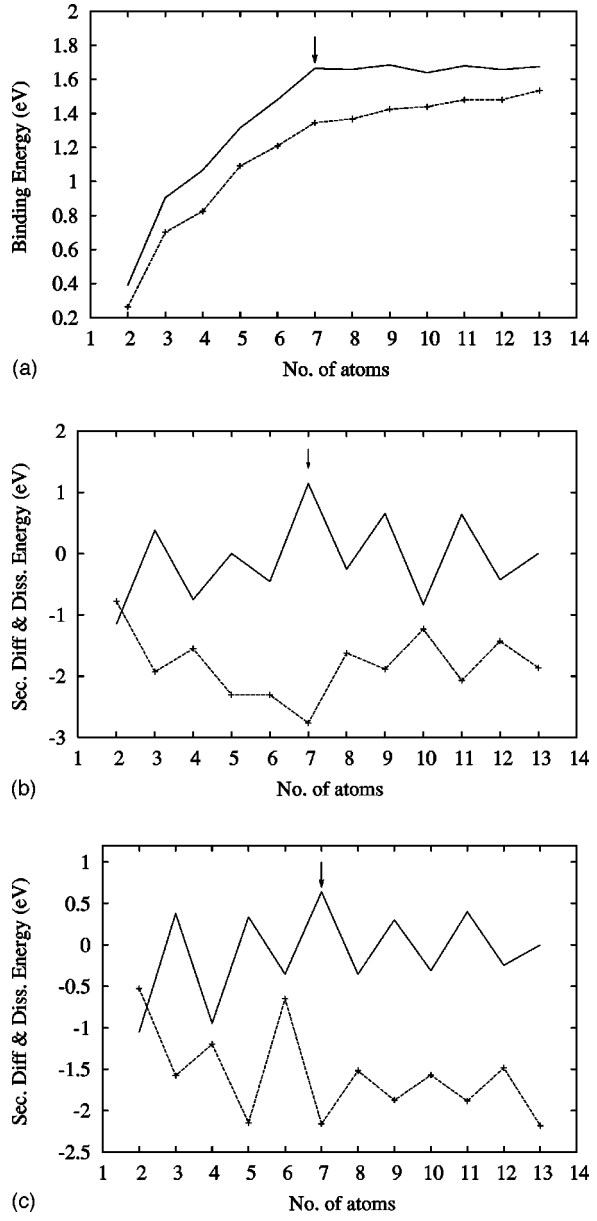

FIG. 3. (a) The binding energy per atom for the Li_nBe (solid line) and the Li_nMg (dotted line) clusters ($n=1$–12) shown as a function of the total number of atoms. The arrow indicates the most stable system with eight valence electrons. (b) The second difference in energy (solid line) and the dissociation energy (dotted line) with respect to the single Li dissociation shown as a function of the total number of atoms for the Li_nBe clusters. The arrow indicates the most stable system with eight valence electrons. (c) The second difference in energy (solid line) and the dissociation energy (dotted line) with respect to the single Li dissociation shown as a function of the total number of atoms for the Li_nMg clusters. The arrow indicates the most stable system with eight valence electrons. All energies are in eV.

eight electron system 10- and 12-electron systems are also stable.

The energy-level diagrams (not shown) of both series show very similar features. The lowest-energy eigenvalue originating from the impurity (s level) is well separated from the rest. After $n=3$, this level shows a delocalized character with a weak p hybridization. The examination of the HOMO-LUMO (lowest unoccupied molecular orbital) gap shows that it is maximum for an eight valence electron system.

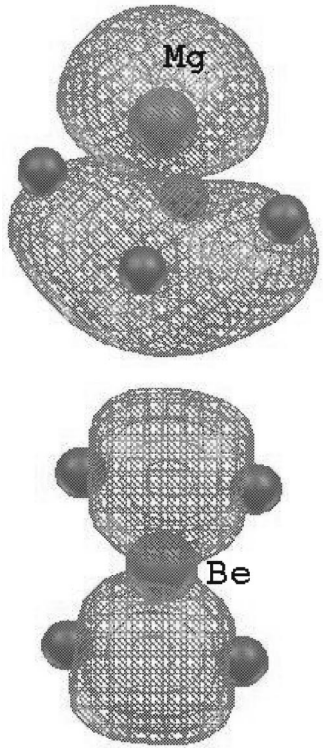

FIG. 4. Isodensity surface corresponding to the highest occupied state (a) for the Li_4Mg cluster, (b) for the Li_4Be cluster.

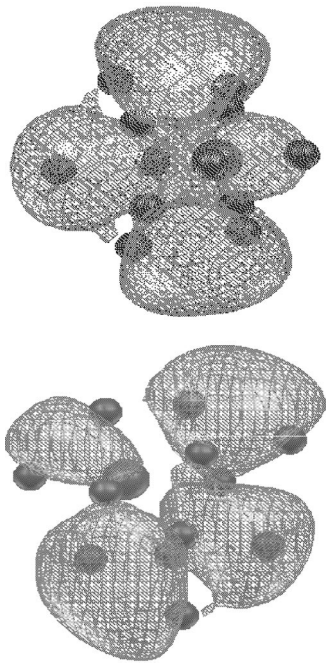

FIG. 5. Isodensity surface corresponding to the highest occupied state (a) for the $Li_{12}Be$ cluster, (b) for the $Li_{12}Mg$ cluster.

Finally we discuss some features of the charge density as seen by an eight-examining isodensities of particular states. We recall that Mg-induced clusters become three-dimensional at $n=4$ as compared to Be-induced ones. This (Li_4Mg) cluster has six electrons and according to SJM should be two-dimensional. The isodensity surfaces for the highest occupied state of Li_4Mg and Li_4Be are shown in Figs. 4(a) and 4(b), respectively. The figure clearly shows the participation of p_z orbital involved with one of the Li atoms in the plane, as indicated by the nodal plane close to the Mg atom. This can be contrasted with the planar ground state of Li_4Be where the highest occupied state is doubly degenerate and involves only p_x and p_y orbitals as expected for the planar structure. Evidently, in the case of Mg, the system lowers the symmetry by lifting the Mg atom above the plane which breaks the doubly degenerate state and brings in the p_z orbital. Another remarkable feature is the very similar character of the *d* complex for larger clusters. Figures 5(a) and 5(b) show the isodensity surfaces for HOMO of $Li_{12}Be$ and $Li_{12}Mg$, respectively. In spite of very different geometries the charge density in both cases shows the nearly identical predominant *d* character. For $n>6$ the calculated electronic-shell structure orders as $1s^2,1p^6,2s^2,1d^{10}$ and the HOMO is neither of pure *s* nor pure *d* type but an admixture of *s* and *d* states.

IV. CONCLUSION

In the present work, we have reported the ground-state geometries of Li_nBe and Li_nMg ($n=1-12$) clusters using the Car-Parrinello molecular-dynamics (CPMD) method. Our geometries obtained by simulated annealing strategy are quite different than those obtained by Fantucci *et al.* [11,12] and Pewestorf *et al.* [13]. Further, it is observed that even though both the impurities are divalent, the ground-state geometries and the growth pattern for both series are different from $n>3$. In the case of Mg, owing to a larger ionic radius than Li weakly interacting Mg does not get trapped in the Li cage. For both series isodensities corresponding to the lowest state show a delocalized character which is dominantly *s* type centered around the impurity.

ACKNOWLEDGMENTS

We gratefully acknowledge partial financial assistance from the Department of Science (New Delhi) and Technology and the Indo-French Center for the Promotion of Advanced Research (New Delhi)/Center Franco-Indian Pour la Promotion de la Recherche Avancee. M.D. acknowledges the University Grants Commission, India and S.C. gratefully acknowledges financial support from CSIR (New Delhi).

[1] *Physics and Chemistry of Finite Systems: From Clusters to Crystals*, edited by P. Jena, S.N. Khanna, and B.K. Rao (Kluwer Academic, Dordrecht, 1992), Vols. 1 and 2; *Clusters and Nanostructured Materials*, edited by P. Jena and S.N. Behera (Nova Science Publishers, Inc., New York, 1996).

[2] W.D. Knight, K. Clemenger, W.A. de Heer, W.A. Saunders, M.Y. Chou, and M.L. Cohen, Phys. Rev. Lett. **52**, 2141 (1984).

[3] M.Y. Chou, M.L. Cohen, Phys. Lett. **113A**, 420 (1986).

[4] M.C. Payne, M.P. Teter, D.C. Allan, T.A. Arias, and J.D. Joannopoulos, Rev. Mod. Phys. **64**, 1045 (1992).

[5] Hai-Ping Cheng, R.N. Barnett, and Uzi Landman, Phys. Rev. B **48**, 1820 (1993).

[6] Ajeeta Dhavale, Vaishali Shah, and D.G. Kanhere, Phys. Rev. A **57**, 4522 (1998).

[7] Ajeeta Dhavale, D.G. Kanhere, C. Majumder, and G.P. Das, Eur. Phys. J. D **6**, 495 (1999).

[8] Rong-qi-TangTang, Phys. Rev. B **43**, 9255 (1991).

[9] U. Röthlisberger and W. Andreoni, Int. J. Mod. Phys. B **6**, 3675 (1992).

[10] S.B. Zang, Marvin L. Cohen and M.Y. Chou, Phys. Rev. B **36**, 3455 (1987).

[11] P. Fantucci, V. Bonačić-Koutecký, and J. Koutecký, Z. Phys. D: At., Mol. Clusters **12**, 307 (1989).

[12] P. Fantucci, V. Bonačić-Koutecký, W. Pewestorf, and J. Koutecký, J. Chem. Phys. **91**, 4229 (1989).

[13] W. Pewestorf, V. Bonačić-Koutecký, and J. Koutecký, J. Chem. Phys. **89**, 5794 (1988).

[14] D.C. Payne and J.D. Joannopoulos, Phys. Rev. Lett. **56**, 2656 (1986).

[15] I. Boustani, W. Pewestorf, P. Fantucci, V. Bonačić-Koutecký, and J. Koutecký, Phys. Rev. B **35**, 9437 (1987).

[16] V. Kumar and R. Car, Phys. Rev. B **44**, 8243 (1991).